DALTON
FULL PAPER

Structural studies of $[Pt(CNMe)_4][M(mnt)_2]_n$ {M = Pd or Pt, mnt = $[S_2C_2(CN)_2]^{2-}$, n = 1 or 2}: structure-dependent paramagnetism of three crystal forms of $[Pt(CNMe)_4][Pt(mnt)_2]_2$

Hugues Bois,[a] Neil G. Connelly,*,†,[a] John G. Crossley,[a] Jean-Christophe Guillorit,[a] Gareth R. Lewis,[a] A. Guy Orpen*,[a] and Peter Thornton[b]

[a] *School of Chemistry, University of Bristol, Bristol, UK BS8 1TS*
[b] *Department of Chemistry, Queen Mary and Westfield College, Mile End Road, London, UK E1 4NS*

The reaction of $[NEt_4]_2[Pt(mnt)_2]$ {mnt = $[S_2C_2(CN)_2]^{2-}$} with $[Pt(CNMe)_4][PF_6]_2$ gave the diamagnetic 'stacked' salt $[Pt(CNMe)_4][Pt(mnt)_2]$. In acetonitrile, nitromethane and nitropropane solution respectively, treatment of $[NEt_4][Pt(mnt)_2]$ with $[Pt(CNMe)_4][PF_6]_2$ yielded three different crystal forms of the salt of 1 : 2 stoichiometry: $[Pt(CNMe)_4][Pt(mnt)_2]_2\cdot 2MeCN$, $[Pt(CNMe)_4][Pt(mnt)_2]_2\cdot MeNO_2$ and $[Pt(CNMe)_4][Pt(mnt)_2]_2$. These show structure-dependent antiferromagnetism, reflecting differing arrangements of the formally platinate(III) anions $[Pt(mnt)_2]^-$ within the crystal lattice. The palladium salts $[Pt(CNMe)_4][Pd(mnt)_2]$ and $[Pt(CNMe)_4][Pd(mnt)_2]_2\cdot 2MeCN$ are isomorphous with their platinum analogues.

Low dimensional molecular solids have attracted widespread interest because of the prospect of novel electrical, optical and magnetic properties. Perhaps the most studied classes of one-dimensional transition metal complexes[1] are the partially oxidised square planar tetracyanoplatinates,[2] *e.g.* $K_2[Pt(CN)_4]Cl_{0.3}\cdot 3H_2O$, and related complexes containing two bidentate dithiolate dianions[3] such as $[S_2C_2(CN)_2]^{2-}$ (mnt).

The structural and physical (electrical conductivity and magnetism) properties of salts of $[M(mnt)_2]^{z-}$ complexes with simple cations such as K^+ and $[NH_4]^+$[4] or organic cations such as that of perylene[5] and [BEDT-TTF]$^+$ [BEDT-TTF = bis(ethylenedithio)tetrathiafulvalene; tetrathiafulvalene = 2-(1,3-dithiol-2-ylidene)-1,3-dithiole][6] have been well studied. By contrast, salts with a transition metal complex as the counter cation are less well known but of obvious potential, as exemplified by [Au(ttp)][M(mnt)$_2$] (M = Ni, Pt or Au; ttp = 5,10,15,20-tetraphenylporphyrinate),[7] $[Fe(\eta\text{-}C_5Me_5)_2][M(mnt)_2]$ (M = Ni or Pt) (which show ferromagnetic behaviour),[8] $[Cr(\eta\text{-}C_6H_6)_2]_2[Ni(mnt)_2]$,[9] $[Fe(\eta\text{-}C_5H_4R)_2]_2[Ni(mnt)_2]$, (R = H[10] or CH=CHC$_6H_4$EMe-4, E = O or S, *etc.*[11]) and $[Fe(\eta\text{-}C_5H_5)(\eta^6\text{-}C_6H_5Me)]_2[Ni(mnt)_2]$.[10,12]

Our preliminary studies[13] in this area showed that the square planar ions $[Pt(CNMe)_4]^{2+}$ and $[M(mnt)_2]^{z-}$ (M = Pd, z = 1 or 2; M = Au, z = 1) give salts with crystal structures which depend on both the charge of the anion and its magnetic state and which show low dimensional motifs (layers and stacks). Here we describe detailed structural and magnetic studies of $[Pt(CNMe)_4][M(mnt)_2]$, $[Pt(CNMe)_4][M(mnt)_2]_2\cdot 2MeCN$ (M = Pd or Pt), $[Pt(CNMe)_4][Pt(mnt)_2]_2\cdot MeNO_2$ and $[Pt(CNMe)_4][Pt(mnt)_2]_2$.

Results and Discussion

Synthesis of complex salts

The salts $[Pt(CNMe)_4][Pt(mnt)_2]$ and $[Pt(CNMe)_4][Pt(mnt)_2]_2$ are prepared by metathesis reactions between $[Pt(CNMe)_4][PF_6]_2$ and 1 equivalent of $[NEt_4]_2[Pt(mnt)_2]$ or 2 equivalents of $[NEt_4][Pt(mnt)_2]$, each dissolved in an appropriate polar solvent. For each complex salt the reaction was carried out in two ways. First, stirring solutions of the reactants together on a preparative scale gave the products as precipitates, generally as powders. Secondly, allowing solutions of the reactants to diffuse together slowly provided crystals suitable for X-ray diffraction studies.

The crystal structure and magnetic behaviour of the products were crucially dependent on solvent incorporation in the lattice. Thus, in the reaction between $[Pt(CNMe)_4][PF_6]_2$ and $[NEt_4][Pt(mnt)_2]$ three crystals forms were isolated, namely $[Pt(CNMe)_4][Pt(mnt)_2]_2\cdot 2MeCN$ (from MeCN), $[Pt(CNMe)_4][Pt(mnt)_2]_2\cdot MeNO_2$ (from $MeNO_2$) and $[Pt(CNMe)_4][Pt(mnt)_2]_2$ (from Pr^nNO_2) (Table 1). Magnetic studies were therefore carried out only on crystalline samples for which the unit cell dimensions of representative single crystals were verified to ensure identity with samples taken for single crystal X-ray diffraction studies.

Crystal structural studies

Aspects of the crystal structures of the salts $[Pt(CNMe)_4][Pt(mnt)_2]$ **1**, $[Pt(CNMe)_4][Pd(mnt)_2]$ **2**,[13] $[Pt(CNMe)_4][Pt(mnt)_2]_2\cdot 2MeCN$ **3**, $[Pt(CNMe)_4][Pd(mnt)_2]_2\cdot 2MeCN$ **4**,[13] $[Pt(CNMe)_4][Pt(mnt)_2]_2\cdot MeNO_2$ **5** and $[Pt(CNMe)_4][Pt(mnt)_2]_2$ **6** are shown in Figs. 1–9; selected structural data are summarised in Table 2.

Molecular structures of the constituent ions. In salts **1**–**6** the diamagnetic dication $[Pt(CNMe)_4]^{2+}$ comprises a square planar d^8 platinum(II) core with nearly linear (apart from the methyl hydrogen atoms) methyl isocyanide ligands; the average Pt–C bond lengths (Table 2) are comparable with that found in $[Pt(CNMe)_4][PF_6]_2$.[14] The bond distances within the square planar anions of **1**–**6** (Table 2) are likewise consistent with those found in the crystal structures of the salts $[NEt_4][Pt(mnt)_2]$[15] and $[NBu^n_4]_2[Pt(mnt)_2]$.[16] Thus, d^8 M^{II}–S bonds are slightly longer than d^7 M^{III}–S bonds. {For simplicity, throughout this paper *formal* oxidation states of II and III are assigned to the metal atoms of $[M(mnt)_2]^{2-}$ and $[M(mnt)_2]^-$ (M = Pd or Pt) respectively.} In other respects the ions have the expected approximately square planar geometry at the metal and there are no substantial distortions of the ligands from their usual dimensions. The Pt atoms in **1**–**3** lie slightly out of the S_4 plane (Table 2) as a result of the 'dish' distortion of the $Pt(mnt)_2$ unit.

† E-Mail: Neil.connelly@bristol.ac.uk

Table 1 Analytical data for complexes **1**–**6**

Complex	State[a]	Colour	Yield (%)	Analysis (%)[b] C	H	N
1 $[Pt(CNMe)_4][Pt(mnt)_2]$	P	Dark red	71	23.2 (23.0)	1.5 (1.5)	13.4(13.4)
	C	Dark red	61	22.9 (23.0)	1.4 (1.5)	13.5(13.4)
2 $[Pt(CNMe)_4][Pd(mnt)_2]$	P	Yellow-green	63	25.6 (25.8)	1.6 (1.6)	14.9(15.0)
	C	Yellow-green	48	26.0 (25.8)	1.4 (1.6)	15.0(15.0)
3 $[Pt(CNMe)_4][Pt(mnt)_2]_2 \cdot 2MeCN$	C	Black	79	24.2 (24.2)	1.2 (1.3)	13.9(14.1)
4 $[Pt(CNMe)_4][Pd(mnt)_2]_2$	P[c]	Black	52	25.0 (25.4)	1.1 (1.1)	14.3(14.8)
5 $[Pt(CNMe)_4][Pt(mnt)_2]_2 \cdot MeNO_2$	C	Black	67	22.1 (21.9)	0.9 (1.1)	13.0(13.3)
6 $[Pt(CNMe)_4][Pt(mnt)_2]_2$	C[d]	Black	25	22.0 (22.0)	1.1 (0.9)	12.8(12.8)

[a] P = Powder, C = crystals. [b] Calculated values in parentheses. [c] Precipitated powder, unresolved. [d] From Pr^nNO_2.

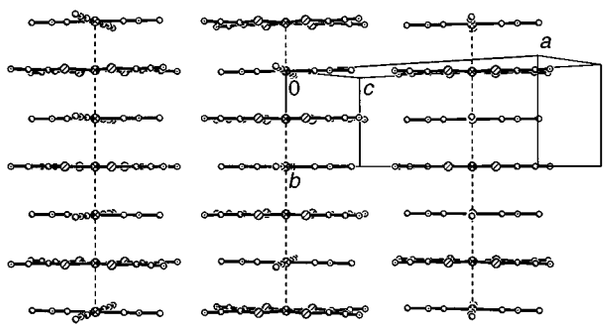

Fig. 1 Crystal structure of complex **1** perpendicular to the *b* axis. Hydrogen atoms have been omitted for clarity

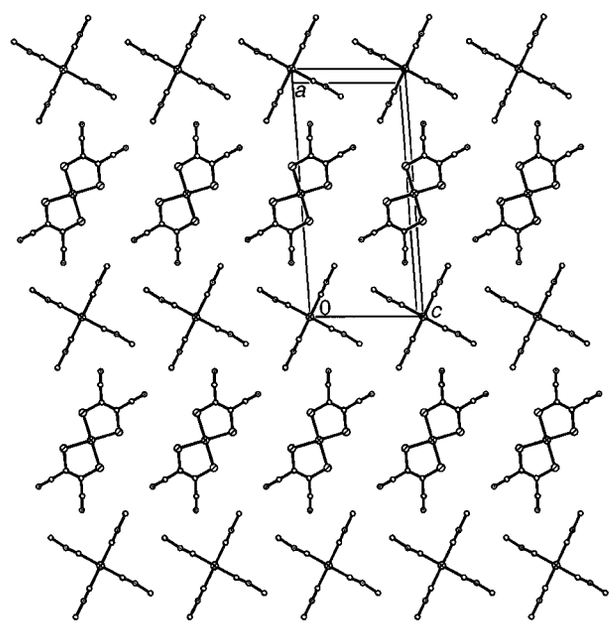

Fig. 2 Crystal structure of complex **1** as viewed along the *b* axis. Details as in Fig. 1

Crystal structures of salts 1–6. The two ions of $[Pt(CNMe)_4][Pt(mnt)_2]$ **1** are arranged such that the metal atoms form an infinite anion–cation one-dimensional stack of type $\ldots A^{2-}C^{2+}A^{2-}C^{2+}A^{2-}C^{2+}\ldots$ (A = anion, C = cation) along the *b* axis (Fig. 1) with a Pt · · · Pt distance of *b*/2, *i.e.* 3.328 Å, and a Pt–Pt–Pt angle of 180°. Ions of like charge have an eclipsed ligand arrangement along the stack. The ions form layers parallel to the *ac* plane of the unit cell (Fig. 2) such that there are segregated homomolecular ribbons of anions and cations along *c*. Each anion is therefore in face-to-face contact with two cations and edge-on contact with two further cations as well as two anions; cations have the converse pattern of contacts. There are also CH · · · N≡C contacts in the layers of *ca.* 2.6 Å.

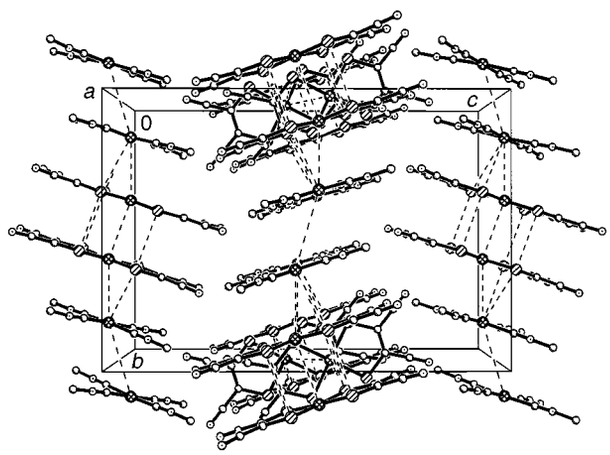

Fig. 3 Crystal structure of complex **3** as viewed along the *a* axis. Solvent and hydrogen atoms have been omitted for clarity

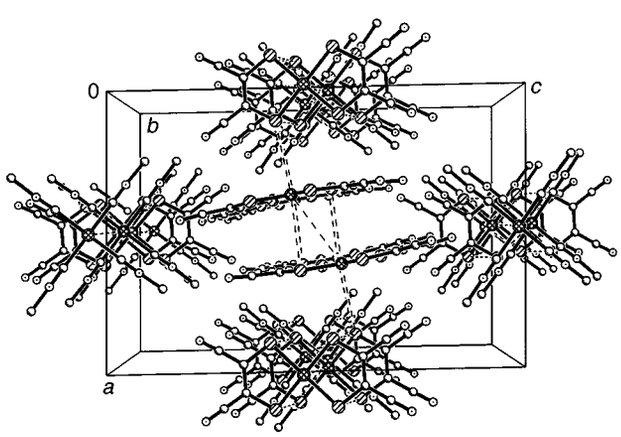

Fig. 4 Crystal structure of complex **3** as viewed along the *b* axis. Details as in Fig. 3

As seen in Table 3, $[Pt(CNMe)_4][Pd(mnt)_2]$ **2** is strictly isostructural with **1**, with palladium atoms replacing platinum in the anions of **1**. The location, site symmetry and geometry of the ions are essentially identical to those described above, with the Pt · · · Pd separation along the metal–metal chain 3.307 Å.

Substituting the diamagnetic d^8 dianions in complexes **1** and **2** by paramagnetic, formally d^7, $[M(mnt)_2]^-$ monoanions causes a change in the stoichiometry of the salt and a dramatic effect on the crystal structure. Moreover, the extensive structural modifications brought about by lattice solvation in the three crystal forms **3**, **5** and **6** result in substantial changes in bulk magnetic behaviour.

The crystal structure of $[Pt(CNMe)_4][Pt(mnt)_2]_2 \cdot 2MeCN$ **3** comprises two separate repeating motifs (Fig. 3) formed by the complex ions in addition to the solvent molecules which lie in

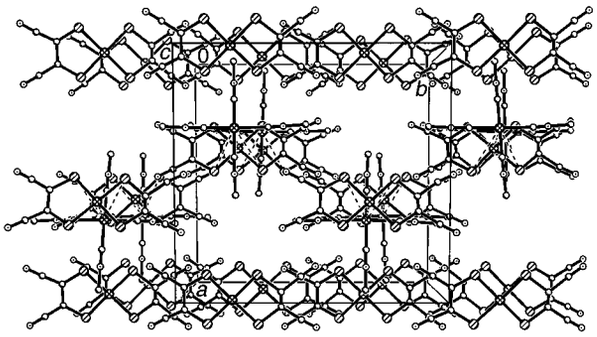

Fig. 5 Crystal structure of complex **5** as viewed along the *c* axis. Details as in Fig. 3

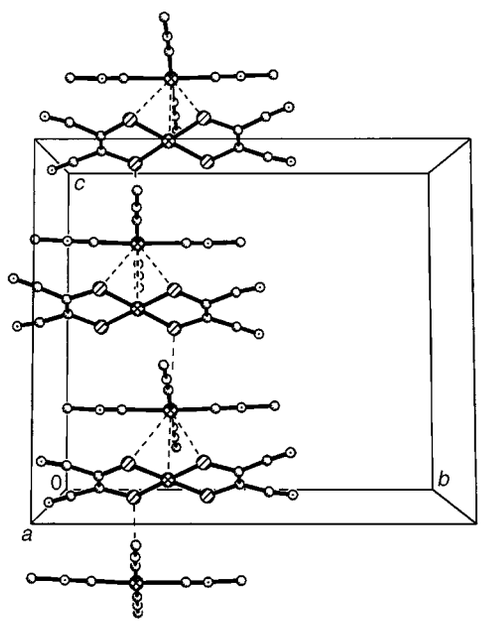

Fig. 6 Cationic chains in the crystal structure of complex **5** as viewed along the *a* axis. Details as in Fig. 3

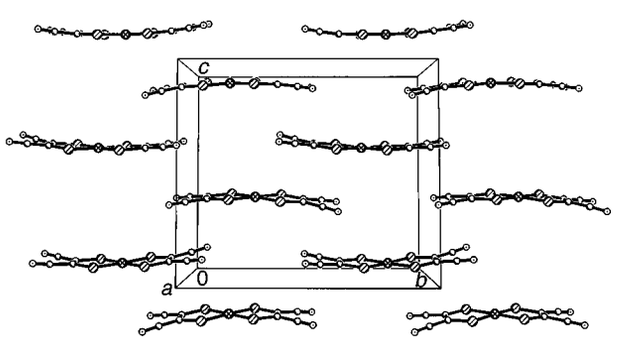

Fig. 7 Anion layers in the *bc* plane in the crystal structure of complex **5** as viewed along the *a* axis. Details as in Fig. 3

the interstices in the array of ions. Face-to-face cationic chains consisting of alternating dication pairs and anion dimers (*i.e.* of type $\ldots A^{-}A^{-}C^{2+}C^{2+}A^{-}A^{-}C^{2+}C^{2+}\ldots$) run along the *b* axis of the crystallographic unit cell at $x = 0$, $z = 0.5$ and $x = 0.5$, $z = 0$. In these chains, the two dications are mutually slipped; the angle of slippage (defined as the angle made by the Pt $\cdots$ Pt vector to the perpendicular to the PtL_4 square plane) is 34.5(4)° and the $Pt^{II} \cdots Pt^{II}$ separation is 4.272(8) Å. Each dication is, in turn, slipped by 22.6(3)° with respect to the neighbouring $[Pt(mnt)_2]^{-}$ anion. The closest $Pt^{II} \cdots Pt^{III}$ separation, between dication and anion, is 3.514(6) Å. The anions in the chain form weak face-to-face dimers with a $Pt^{III} \cdots Pt^{III}$ separation of

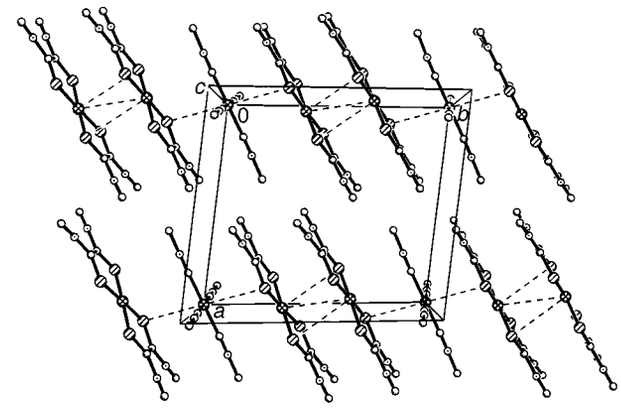

Fig. 8 Neutral chains along the *b* axis of the crystal structure of complex **6** as viewed along the *c* axis. Details as in Fig. 1

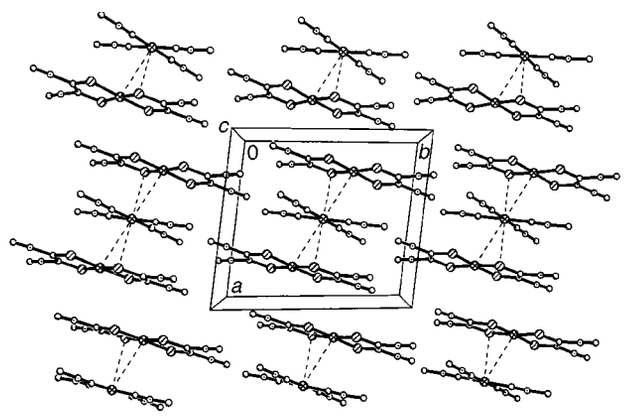

Fig. 9 Neutral chains along the *a* axis of the crystal structure of complex **6** as viewed along the *c* axis. Details as in Fig. 1

3.507(6) Å; the angle of slippage is only 1.6(2)°, *i.e.* the anions are nearly perfectly eclipsed. The *b*-axis chains are linked by weak Pt $\cdots$ S contacts [3.860(6) Å] (Fig. 4) to anion dimers which are similar to those in the *b*-axis chain but more internally slipped, so giving a much greater intradimer Pt $\cdots$ Pt distance [4.252(8) Å] and an angle of slippage of 28.6(3)°.

Substituting the d^7 platinate anion $[Pt(mnt)_2]^{-}$ of complex **3** by the d^7 palladate anion $[Pd(mnt)_2]^{-}$ of **4** has little effect on the overall crystal structure. As seen in Table 3 crystals of the two salts, as their acetonitrile solvates, are strictly isostructural. The palladium–palladium distances in **4** within the two types of anion dimer are slightly shorter [*i.e.* Pd $\cdots$ Pd 3.421(5) Å (in the *b*-axis chain) and 4.240(6) Å (in the isolated dimers)] than in the corresponding platinum anion pairs.

As seen in Figs. 5 and 6, the solvation of $[Pt(CNMe)_4][Pt(mnt)_2]_2$ by $MeNO_2$ in **5** (*cf.* 2MeCN in **3**) results in a markedly different structure. The crystal structure of **5** contains two types of ion arrangement. Chains of alternating $[Pt(mnt)_2]^{-}$ and $[Pt(CNMe)_4]^{2+}$ ions, of the form $\ldots A^{-}C^{2+}A^{-}C^{2+}A^{-}C^{2+}\ldots$, may be observed parallel to the *c* axis (Figs. 5 and 6). In these cationic chains, therefore, the paramagnetic anions are isolated from other paramagnetic centres. One sulfur of the anion is closest to the metal atom of the adjacent dication, at a distance of 3.657(8) Å and with an angle of slippage of 16.6(3)°. In turn, the metal atom of the dication lies 3.310(7) Å above the platinum of the next neighbouring anion. In addition a layer of $[Pt(mnt)_2]^{-}$ anions is formed in the *bc* plane at $x = 0$, 1, 2, *etc.* (Fig. 7) in which the anions lie face-to-face, forming an array in which highly slipped 'chains' may be identified with closest $Pt^{III} \cdots Pt^{III}$ separations of 7.454(7) and 7.582(8) Å. However, there are shorter $Pt^{III} \cdots Pt^{III}$ contacts (6.641 Å) between anions in the chains and layers. Thus, there are two different magnetic

Table 2 Selected average bond and interatomic lengths (Å) and angles (°) for complexes **1**–**6**

Cation	**1**	**2**	**3**	**4**	**5**	**6**
Average Pt^{II}–C [a]	1.991(4) [b]	1.968(6)	1.972(12)	1.979(1)	2.005(5)	1.957(2)
Average *cis* C–Pt^{II}–C	89.50(2)	90.00(1)	88.4(4)	90.0(1)	90.00(8)	91.32(3)
Average Pt^{II}–N–C	175.7(4)	179.4(2)	172.0(7)	177.4(1)	177.9(8)	176.1(2)
Anion						
Average M–S [c]	2.311(1)	2.304(2)	2.271(2)	2.275(1)	2.268(3)	2.257(3)
Average *cis* S–M–S	90.2(2)	90.0(2)	90.0(7)	90.0(3)	90.1(6)	90.0(1)
Deviation of M from MS_4	0.0(0)	0.0(0)	0.0303(4)	0.0351(3)	0.0860(3)	0.0270(2)
square plane			0.0299(4)	0.0245(3)	0.0340(2)	0.0170(2)

[a] Literature value = 1.980 Å.[14] [b] Typical standard uncertainties in the last digit of individual values are given in parentheses. [c] Literature values: Pt–S in $[Pt(mnt)_2]^-$ 2.266 Å;[15] in $[Pt(mnt)_2]^{2-}$ 2.283 Å;[16] Pd–S in $[Pd(mnt)_2]^-$ 2.278 Å.[4c]

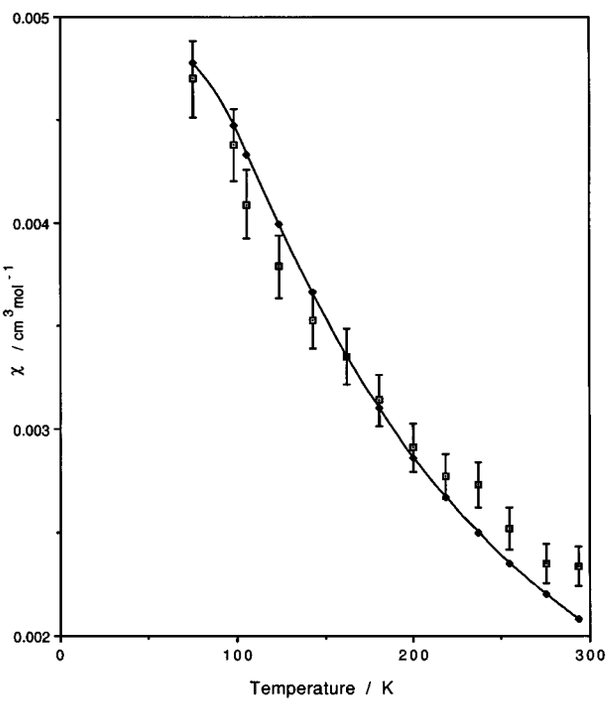

Fig. 10 Magnetic susceptibility *vs.* temperature for complex **3**. Experimental points, squares; calculated values, filled circles and line, see text

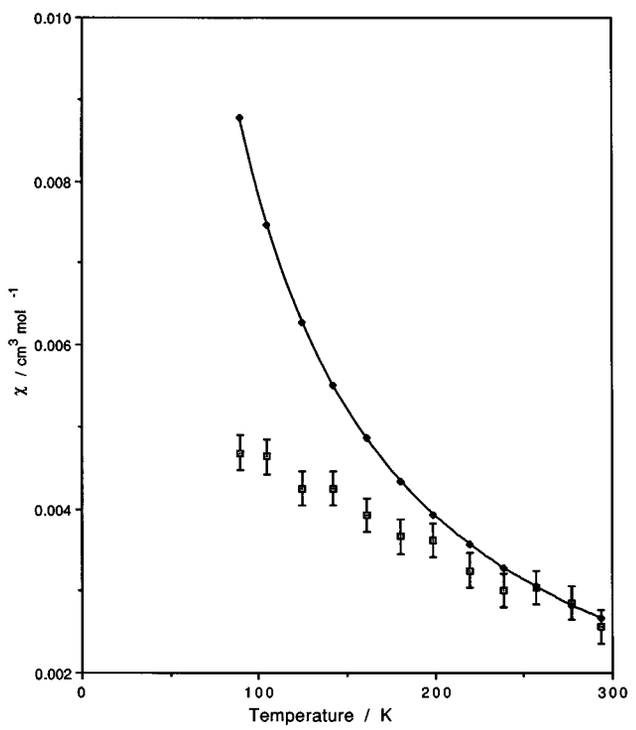

Fig. 11 Magnetic susceptibility *vs.* temperature for complex **6**. Details as in Fig. 10

environments for the platinum(III) centres within the crystals of **5** (see below) and the large separations between the paramagnetic centres seem likely to provide an insulating environment for the anions. As in **4** the solvent molecules lie in the interstices of the array of ions in **5**.

The unsolvated crystal structure of complex **6** (Figs. 8 and 9) once again contains anion dimers. However, in this case the dimers are separated only by single dications thereby forming neutral chains of the form ... $A^-A^-C^{2+}A^-A^-C^{2+}A^-A^-C^{2+}$.... Two such chains are formed, one parallel to the *b* axis and a second, more weakly associated, along the *a* axis. In the *b* axis chain (Fig. 8) the dimers are only slightly slipped, at an angle of 7.2(3)°, and the $Pt^{III} \cdots Pt^{III}$ distance is 3.859(8) Å. The $[Pt(CNMe)_4]^{2+}$ dication is slightly staggered with respect to the anion dimer, and aligned such that the platinum(II) centre is below the sulfur atom of an mnt ligand, at a Pt ··· S distance of 3.490(8) Å, and at an angle of slippage of 14.2(3)°. In the *a* axis chain (Fig. 9) the $Pt^{III} \cdots Pt^{III}$ distance is longer and more slipped [at 5.433(7) Å and 19.2(3)°] and the $Pt^{II} \cdots Pt^{III}$ distance shorter and less slipped [at 3.742(5) Å and 17.1(3)°].

Magnetic susceptibility studies on $[Pt(CNMe)_4][Pt(mnt)_2]_2 \cdot 2MeCN$ 3, $[Pt(CNMe)_4][Pt(mnt)_2]_2 \cdot MeNO_2$ 5 and $[Pt(CNMe)_4][Pt(mnt)_2]_2$ 6

The magnetic susceptibilities of the salts **3**, **5** and **6** were measured by the Faraday method from 74 to 294 K. The χ *vs.* *T* plots are shown in Figs. 10–12. Temperature independent paramagnetism is accounted for by the inclusion of a correction term, $8N\beta^2/\Delta$, with Δ for $[Pt(mnt)_2]^-$ measured from the electronic spectrum as 11 700 cm^{-1},[3a] giving a second order molar susceptibility of 1.80×10^{-4} cm^3 mol^{-1}.

Each of the crystal forms is antiferromagnetic, but the extent of antiferromagnetism reflects the different structures. The bis(acetonitrile) solvate **3** contains two types of well separated platinate(III) anion dimers (see above, Figs. 3 and 4). Its magnetism is well described using the Bleaney–Bowers equation[17] with a value of *J*, the magnetic interaction parameter, of -80 cm^{-1} (Fig. 10). A value of 2.000 was assumed for *g*; a higher value to include some spin–orbit coupling gives a poorer fit below 150 K. The fit of theory to experiment is

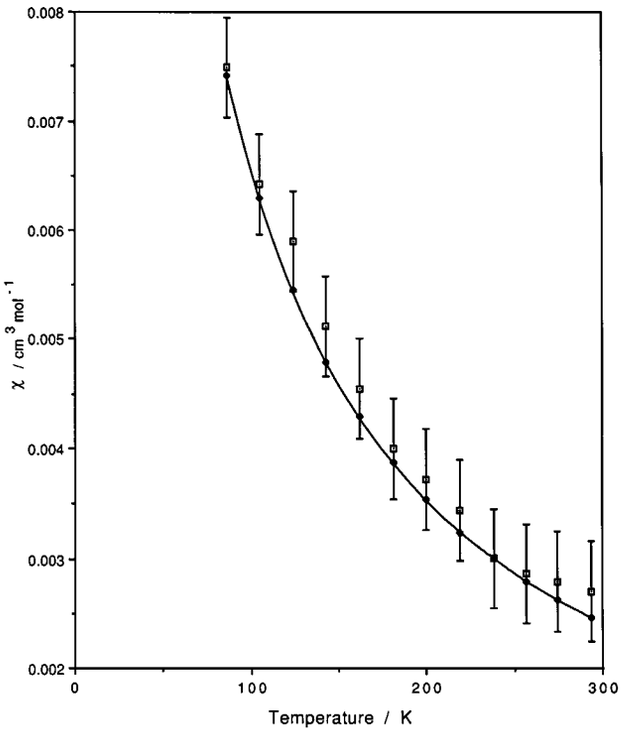

Fig. 12 Magnetic susceptibility *vs.* temperature for complex **5**. Details as in Fig. 10

not exact, but in the available temperature range all the experimental points are within two standard deviations of the theoretical curve.

Compound **6**, the unsolvated salt obtained from nitropropane solution, also contains platinate(III) anion dimers (albeit of two markedly different types in approximately orthogonal chains) and might therefore be expected to show similar behaviour to that of **3**. However, it can be seen from Fig. 11 that the susceptibility decreases more rapidly at lower temperatures than the Bleaney–Bowers theory for an $S = \frac{1}{2}$ dimer predicts, using the best J value of -135 cm^{-1}. This may be attributed to the possibility of interdimer coupling to give an alternating chain with additional antiferromagnetism between dimeric anions through orbital overlap with the dications. This additional antiferromagnetism will be more prominent at lower temperatures. It is noteworthy that the intradimer coupling constant in **6** is much greater than for **3**, despite the distance between platinum(III) atoms being much longer. It may be that for **6** exchange mediated through the dication is greater in magnitude than that between two anions which are not apparently insulated by a dication and that, magnetically speaking, **6** should be considered as a dimer of monoanions bridged by a dication. We consider it premature to compute an additional exchange parameter to represent the minor coupling in advance of data for lower temperatures; these might well give a maximum in the susceptibility *vs.* temperature curve at about 50 K.

The nitromethane solvate **5** contains a polymeric layer of face-to-face platinum(III) ions, each with spin of $\frac{1}{2}$, with additional separate platinate(III) anions in the cationic stack. For an infinite chain of spins of $\frac{1}{2}$ interacting antiferromagnetically the formula derived by Bonner and Fisher[18] applies [equation (1)]

$$\chi = \frac{N_a g^2 \beta^2}{kT} \frac{0.25 + 0.074\,974x + 0.075\,235x^2}{1.0 + 0.9931x + 0.172\,135x^2 + 0.757\,825x^3} \quad (1)$$

where $x = J/kT$. The susceptibility of the salt is found by adding the susceptibility given by equation (1) to that for an isolated ion of spin $\frac{1}{2}$. It can be seen from Fig. 12 that a satisfactory fit to the data can be obtained using a value of J of -39 cm^{-1}.

It is notable that the different polymeric array of complex **5** gives antiferromagnetism of the same order as that of the dimer-based antiferromagnets **3** and **6**. However, the values of J obtained are not really comparable, as they are obtained from different equations and probably arise from different combinations of orbital overlaps. The remote Pt···Pt separations in **5** imply interaction through overlaps with cations, but the much shorter contacts in **3** and **6** suggest that some direct overlap of magnetic orbitals on Pt is possible for these salts. Any superexchange pathways will be different in all three compounds.

Experimental

The preparation, purification and reactions of the complexes described were carried out under an atmosphere of dry nitrogen using dried, distilled and deoxygenated solvents. Unless stated otherwise, the complex salts are air-stable in the solid state and are insoluble in all common organic solvents. The complexes $[Pt(CNMe)_4][PF_6]_2$,[19] $[NEt_4]_2[Pt(mnt)_2]$,[20] $[NEt_4][Pt(mnt)_2]$,[21] $[NBu^n_4]_2[Pd(mnt)_2]$[20] and $[NBu^n_4][Pd(mnt)_2]$[21] were prepared by published methods. Microanalyses were carried out by the staff of the Microanalytical Service of the School of Chemistry, University of Bristol.

Preparations

$[Pt(CNMe)_4][Pt(mnt)_2]$ 1. (*a*) *Powder*. The complex $[NEt_4]_2[Pt(mnt)_2]$ (0.111 g, 0.151 mmol) in MeCN (10 cm^3) was added to a stirred solution of $[Pt(CNMe)_4][PF_6]_2$ (0.101 g, 0.156 mmol) in MeCN (10 cm^3). After 40 min the red solid was removed by filtration, washed with diethyl ether and dried in air, yield 0.09 g (71%).

(*b*) *Crystals*. To a solution of $[Pt(CNMe)_4][PF_6]_2$ (25 mg, 0.039 mmol) in MeCN (10 cm^3) in a 2 cm diameter Schlenk tube was carefully added $[NEt_4]_2[Pd(mnt)_2]$ (28 mg, 0.040 mmol) in MeCN (10 cm^3) to form two layers. After the two layers had diffused together for 2 d the dark red crystals were collected, washed with acetonitrile (10 cm^3) and diethyl ether (10 cm^3) and then dried in air, yield 20 mg (61%).

The salt $[Pt(CNMe)_4][Pd(mnt)_2]$ **2** was prepared similarly, as yellow-green needles, from $[Pt(CNMe)_4][PF_6]_2$ and $[NBu^n_4]_2[Pd(mnt)_2]$.

$[Pt(CNMe)_4][Pt(mnt)_2]_2 \cdot 2MeCN$ 3. To a solution of $[Pt(CNMe)_4][PF_6]_2$ (0.160 g, 0.246 mmol) in MeCN (25 cm^3) in a 5 cm diameter Schlenk tube was carefully added $[NEt_4][Pt(mnt)_2]$ (0.298 g, 0.492 mmol) in MeCN (25 cm^3) to form two layers. After diffusion for 1 month, the product was obtained as black diamond-shaped crystals which were washed with MeCN and then diethyl ether and dried in air, yield 0.270 g (79%).

The salt $[Pt(CNMe)_4][Pd(mnt)_2]_2 \cdot 2MeCN$ **4** was prepared similarly. The complex $[Pt(CNMe)_4][Pt(mnt)_2]_2 \cdot MeNO_2$ **5** was obtained by the same method, in $MeNO_2$, as large black needles after 2 d in 67% yield (after washing the crystals with $MeNO_2$ and diethyl ether); $[Pt(CNMe)_4][Pt(mnt)_2]_2$ **6** was obtained by the same method, in Pr^nNO_2, as black cubes after 2 d in 25% yield (after washing the crystals with Pr^nNO_2 and diethyl ether).

Magnetic studies

Magnetic susceptibilities were determined by the Faraday technique using apparatus and methods described earlier.[22] Owing to the large diamagnetic corrections and low susceptibilities of the compounds the experimental error in susceptibility is rather higher than normal, being ±4% for **3**, ±3% for **5** and ±7% for **6**.

Crystallography

Crystal data and other details of the structure analyses are presented in Table 3. For complex **4** difference electron density

Table 3 Crystal and refinement data for complexes **1**–**6**

Salt	**1**	**2**	**3**	**4**	**5**	**6**
Empirical formula	$C_{16}H_{12}N_8Pt_2S_4$	$C_{16}H_{12}N_8PdPtS_4$	$C_{28}H_{18}N_{14}Pt_3S_8$	$C_{24}H_{18}N_{14}Pd_2PtS_8$	$C_{25}H_{15}N_{13}O_2Pt_3S_8$	$C_{24}H_{12}N_{12}Pt_3S_8$
M	834.76	746.06	1392.30	1214.93	1371.23	1310.19
T/K	298(5)	298(5)	298(5)	298(5)	173(2)	173(2)
Crystal system	Monoclinic	Monoclinic	Monoclinic	Monoclinic	Monoclinic	Triclinic
Space group (no.)	$C2/m$ (12)	$C2/m$ (12)	$P2_1/n$ (14)	$P2_1/n$ (14)	$P2_1/c$ (14)	$P\bar{1}$ (2)
a/Å	20.000(7)	19.933(4)	14.071(4)	14.063(6)	15.913(3)	11.069(2)
b/Å	6.655(3)	6.614(1)	14.414(4)	14.385(6)	16.807(3)	12.463(3)
c/Å	9.182(4)	9.152(3)	20.747(6)	20.668(9)	14.799(3)	13.514(3)
α/°						100.323(10)
β/°	94.13(3)	94.09(2)	91.16(2)	91.28(3)	96.417(3)	91.272(12)
γ/°						96.547(11)
U/Å^3	1219.0(9)	1203.5(5)	4208.0(21)	4180.0(31)	3933.1(9)	1820.5(7)
Z	2	2	4	4	4	2
μ/mm^{-1}	11.83	6.92	10.39	4.63	11.11	11.99
Reflections collected	2656	2191	11 430	7349	14 791	7818
Independent reflections	1760	1475	8707	5409	5600	5103
R_{int}	0.0633	0.0246	0.0528	0.0310	0.0779	0.0585
Final $R1$ [$I > 2\sigma(I)$], $wR2$	0.0499, 0.0959	0.0329, 0.0813	0.0546, 0.1044	0.0465, 0.0990	0.0677, 0.1542	0.0493, 0.1247

close to the weakly dimerised $[Pd(mnt)_2]^-$ anions in the columnar stacks making four short contacts of *ca.* 2.3 Å could be modelled as an oxygen atom, or more satisfactorily, as a low occupancy disordered [0.103(3)] orientation of the Pd(2) atom in the dimer. The second orientation, in which the dimer is rotated by 90° about its longest axis, apparently occupies a very similar volume and shape as the first. Acetonitrile hydrogens were refined in idealised geometries (C–H 0.96 Å, H–C–H 109.5°, free rotation about the C–Me bond).

CCDC reference number 186/1060.

See http://www.rsc.org/suppdata/dt/1998/2833/ for crystallographic files in .cif format.

Acknowledgements

We thank the EPSRC for research studentships (to J. G. C. and G. R. L.).

References

1 See, for example, *Inorganic Materials*, eds. D. W. Bruce and D. O'Hare, Wiley, New York, 1992; *Extended Linear Chain Compounds*, ed. J. S. Miller, Plenum, New York, 1992; J. S. Miller and A. J. Epstein, *Prog. Inorg. Chem.*, 1976, **20**, 1.
2 J. M. Williams, *Adv. Inorg. Chem. Radiochem.*, 1983, **26**, 235; K. Krogmann, *Angew. Chem., Int. Ed. Engl.*, 1969, **8**, 35.
3 (*a*) J. A. McCleverty, *Prog. Inorg. Chem.*, 1968, **10**, 49; (*b*) R. P. Burns and C. A. McAuliffe, *Adv. Inorg. Chem. Radiochem.*, 1979, **22**, 303.
4 (*a*) A. T. Coomber, D. Beljonne, R. H. Friend, J. L. Bredas, A. Charlton, N. Robertson, A. E. Underhill, M. Kurmoo and P. Day, *Nature* (*London*), 1996, **380**, 144; (*b*) P. I. Clemenson, *Coord. Chem. Rev.*, 1990, **106**, 171; (*c*) M. B. Hursthouse, R. L. Short, P. I. Clemenson and A. E. Underhill, *J. Chem. Soc.*, *Dalton Trans.*, 1989, 67; (*d*) M. B. Hursthouse, R. L. Short, P. I. Clemenson and A. E. Underhill, *J. Chem. Soc.*, *Dalton Trans.*, 1989, 1101.
5 L. Alcacar and A. H. Maki, *J. Phys. Chem.*, 1974, **78**, 215; 1976, **80**, 1912; A. Domingos, R. T. Henriques, V. Gama, M. Almeida, A. Lopes Vieira and L. Alcacer, *Synth. Metals*, 1988, **27**, B411; R. T. Henriques, V. Gama, G. Bonfait, I. C. Santos, M. J. Matos, M. Almeida, M. T. Duarte and L. Alcacer, *Synth. Metals*, 1993, **56**, 1846; V. Gama, R. T. Henriques, G. Bonfait, L. C. Pereira, J. C. Waerenborgh, I. C. Santos, M. T. Duarte, J. M. P. Cabral and M. Almeida, *Inorg. Chem.*, 1992, **31**, 2598; V. Gama, R. T. Henriques, G. Bonfait, M. Almeida, A. Meetsma, S. van Smaalen and J. L. de Boer, *J. Am. Chem. Soc.*, 1992, **114**, 1986.
6 W. Reith, K. Polborn and E. Amberger, *Angew. Chem.*, *Int. Ed. Engl.*, 1988, **27**, 699.
7 Z. J. Zhong, H. Okawa, R. Aoki and S. Kida, *Inorg. Chim. Acta*, 1988, **144**, 233.
8 J. S. Miller, J. C. Calabrese and A. J. Epstein, *Inorg. Chem.*, 1989, **28**, 4230.
9 E. Polo, M. Scoponi, S. Sostero, J. Szklarewics and O. Traverso, *Gazz. Chim. Ital.*, 1994, **124**, 503.
10 J. Qin, Y. Ding, W. Zhou and D. Liu, *Huaxue Xuebao*, 1993, **51**, 202 (*Chem. Abstr.*, 1993, **119**, 95 750).
11 M. Hobi, S. Zurcher, V. Gramlich, U. Burckhardt, C. Mensing, M. Spahr and A. Togni, *Organometallics*, 1996, **15**, 5342.
12 J. G. Qin, W. H. Zhou, C. L. Yang, D. Y. Liu, N. H. Hu and Z. S. Jin, *Synth. Metals*, 1995, **70**, 1217.
13 N. G. Connelly, J. G. Crossley, A. G. Orpen and H. Salter, *J. Chem. Soc.*, *Chem. Commun.*, 1992, 1564.
14 J. G. Crossley and A. G. Orpen, *Acta Crystallogr.*, *Sect. C*, 1995, **51**, 1102.
15 P. I. Clemenson, A. E. Underhill, M. B. Hursthouse and R. L. Short, *J. Chem. Soc.*, *Dalton Trans.*, 1989, 61.
16 W. Guntner, G. Gliemann, U. Klement and M. Zabel, *Inorg. Chim. Acta*, 1989, **165**, 51.
17 B. Bleaney and K. D. Bowers, *Proc. R. Soc. London*, *Ser. A*, 1952, **214**, 451.
18 J. C. Bonner and M. E. Fisher, *Phys. Rev. A*, 1964, **135**, 640.
19 J. S. Miller and A. L. Balch, *Inorg. Chem.*, 1972, **11**, 2069.
20 A. Davison, N. Edelstein, R. H. Holm and A. H. Maki, *Inorg. Chem.*, 1963, **2**, 1227.
21 J. F. Weiher, L. R. Melby and R. E. Benson, *J. Am. Chem. Soc.*, 1964, **86**, 4329.
22 M. A. Laffey and P. Thornton, *J. Chem. Soc.*, *Dalton Trans.*, 1982, 313.

Received 8*th May* 1998; *Paper* 8/03456G